On evaluation of transverse spin fluctuations in quantum magnets

Avinash Singh
Department of Physics, Indian Institute of Technology, Kanpur-208016, India

A numerical method is described for evaluating transverse spin correlations in the random phase approximation. Quantum spin-fluctuation corrections to sublattice magnetization are evaluated for the antiferromagnetic ground state of the half-filled Hubbard model in two and three dimensions in the whole U/t range. Extension to the case of defects in the AF is also discussed for spin vacancies and low$-U$ impurities. In the $U/t \to \infty$ limit, the vacancy-induced enhancement in the spin fluctuation correction is obtained for the spin-vacancy problem in two dimensions, for vacancy concentration up to the percolation threshold. For low-U impurities, the overall spin fluctuation correction is found to be strongly suppressed, although surprisingly spin fluctuations are locally enhanced at the low$-U$ sites.

75.10.Jm, 75.10.Lp, 75.30.Ds, 75.10.Hk

I. INTRODUCTION

Transverse spin fluctuations are gapless, low-energy excitations in the broken-symmetry state of magnetic systems possessing continuous spin-rotational symmetry. Therefore at low temperatures they play an important role in diverse macroscopic properties such as existence of long-range order, magnitude and temperature-dependence of the order parameter, Néel temperature, spin correlations etc. Specifically in the antiferromagnetic (AF) ground state of the half-filled Hubbard model transverse spin fluctuations are important both in two and three dimensions, where antiferromagnetic long-range order (AFLRO) exists at $T = 0$. In the strong-coupling limit ($U/t \to \infty$), where spin fluctuations are strongest, they significantly reduce the zero-temperature AF order parameter in two dimensions to nearly 60% of the classical (HF) value. [1–4] Similarly the Néel temperature in three dimensions is reduced to nearly 65% of the mean-field result $T_{\rm N}^{\rm MF} = zJ/4 = 6t^2/U$, for the equivalent $S = 1/2$ quantum Heisenberg antiferromagnet (QHAF). [5]

Recently there has also been interest in spin fluctuations due to defects, disorder and vacancies in the quantum antiferromagnet. In the random-U model, where U is set to zero on a fraction f of sites, the lattice-averaged AF order parameter appears to be enhanced for small f, as seen in QMC calculations, [6] presumably due to an overall suppression of quantum spin fluctuations. On the other hand spin fluctuations are enhanced by strong disorder in the Hubbard model with random on-site energies. In the strong disorder regime, overlap of the two Hubbard bands leads to formation of essentially empty and doubly-occupied sites, which act like spin vacancies. [7] The problem of spin vacancies in the quantum antiferromagnet is also relevant to the electron-doped materials like $Nd_{2-x}Ce_xCuO_4$, where spin-dilution behavior is observed. [8,9] While the problem of magnon energy renormalization due to spin vacancies has been addressed recently, [10–15] these methods are limited to the low-concentration limit, and the vacancy-induced enhancement in transverse spin fluctuations has not been studied in the whole range of vacancy concentration.

In this paper we describe a new method for evaluating transverse spin correlations and quantum spin-fluctuation corrections about the HF-level broken-symmetry state, in terms of magnon mode energies and spectral functions obtained in the random phase approximation (RPA). The method is applicable in the whole U/t range of interaction strength, and is illustrated with three applications involving the AF ground state of the half-filled Hubbard model — (i) the pure model in $d = 2, 3$, (ii) spin vacancies in the strong coupling limit in $d = 2$, and (iii) low-U impurities in $d = 2$. This method for obtaining quantum correction to sublattice magnetization solely in terms of transverse spin correlations is parallel to the spin-wave-theory (SWT) approach, [16,17] and differs from the method involving self-energy corrections. [18]

The RPA approach has been demonstrated earlier to properly interpolate between the weak and strong coupling limits for the spin-wave velocity. [3,18] By going beyond the RPA level within a systematic inverse-degeneracy expansion scheme, which preserves the spin-rotational symmetry and hence the Goldstone mode order by order, it was also shown that in the strong coupling limit identical results are obtained for all quantum corrections, order by order, as from the SWT approach for the QHAF. [4] A renormalized RPA approach has also been devised recently to obtain the magnetic phase diagram for the three dimensional Hubbard model in the whole U/t range, and the $T_{\rm N}$ vs. U behaviour was shown to properly interpolate between the weak and strong coupling limits. [5]

II. TRANSVERSE SPIN CORRELATIONS

The method is based on a convenient way to perform the frequency integral in order to obtain spin correlations from spin propagators, and we illustrate it here

for transverse spin correlations. We write the time-ordered, transverse spin propagator for sites i and j, $\langle\Psi_{\rm G}|T[S_i^-(t)S_j^+(t')]|\Psi_{\rm G}\rangle$ at the RPA level in frequency space as,

$$[\chi^{-+}(\omega)] = \frac{[\chi^0(\omega)]}{1-U[\chi^0(\omega)]} = \sum_n \frac{\lambda_n(\omega)}{1-U\lambda_n(\omega)}|\phi_n(\omega)\rangle\langle\phi_n(\omega)| \ , \tag{1}$$

where $|\phi_n(\omega)\rangle$ and $\lambda_n(\omega)$ are the eigenvectors and eigenvalues of the $[\chi^0(\omega)]$ matrix. Here $[\chi^0(\omega)]_{ij} = i\int(d\omega'/2\pi)G^{\uparrow}_{ij}(\omega')G^{\downarrow}_{ji}(\omega'-\omega)$ is the zeroth-order, antiparallel-spin particle-hole propagator, evaluated in the self-consistent, broken-symmetry state from the HF Green's functions $G^\sigma(\omega)$. Spin correlations are then obtained from,

$$\begin{aligned}\langle S_i^-(t)S_j^+(t')\rangle_{\rm RPA} &= -i\int\frac{d\omega}{2\pi}[\chi^{-+}(\omega)]_{ij}\ e^{-i\omega(t-t')} \\ &= \pm\sum_n \frac{\phi_n^i(\omega_n)\phi_n^j(\omega_n)}{U^2(d\lambda_n/d\omega)_{\omega_n}}e^{-i\omega_n(t-t')} \ , \end{aligned} \tag{2}$$

where the collective mode energies ω_n are obtained from $1-U\lambda_n(\omega_n)=0$, and $\lambda_n(\omega)$ has been Taylor-expanded as $\lambda_n(\omega)\approx\lambda_n(\omega_n)+(\omega-\omega_n)(d\lambda_n/d\omega)_{\omega_n}$ near the mode energies to obtain the residues. For convergence, the retarded (advanced) part of the time-ordered propagator χ^{-+}, having pole below (above) the real-ω axis, is to be taken for $t'<t$ ($t'>t$). The frequency integral is conveniently replaced by an appropriate contour integral in the lower or upper half-plane in the complex-ω space for these two cases, respectively, which results in Eq. (2).

III. HUBBARD MODEL IN D = 2,3

We first illustrate this method for the half-filled Hubbard model in two and three dimensions on square and simple-cubic lattices, respectively. In this case it is convenient to use the two-sublattice representation due to translational symmetry, and we work with the 2×2 matrix $[\chi^0(q\omega)]$ in momentum space, which is given in terms of eigensolutions of the HF Hamiltonian matrix. [3] The k-summation is performed numerically using a momentum grid with $\Delta k = 0.1$ and 0.05, in three and two dimensions, respectively.

Equal-time, same-site transverse spin correlations are then obtained from Eq. (2) by summing over the different q modes, using a momentum grid with $\Delta q = 0.3$ and 0.1 in three and two dimensions, respectively. We consider $t'\to t^-$, so that the retarded part is used, with positive mode energies. From spin-sublattice symmetry, correlations on A and B sublattice sites are related via $\langle S^+S^-\rangle_A = \langle S^-S^+\rangle_B$. Thus the transverse spin correlations are obtained from magnon amplitudes on A and B sublattices, and from Eq. (2) we have

$$\begin{aligned}\langle S^-S^+\rangle_{\rm RPA} &= \sum_q \frac{(\phi_q^A)^2}{U^2(d\lambda_q/d\omega)_{\omega_q}} \\ \langle S^+S^-\rangle_{\rm RPA} &= \sum_q \frac{(\phi_q^B)^2}{U^2(d\lambda_q/d\omega)_{\omega_q}} \ . \end{aligned} \tag{3}$$

From the commutation relation $[S^+,S^-]=2S^z$, the difference $\langle S^+S^- - S^-S^+\rangle_{\rm RPA}$, of transverse spin correlations evaluated at the RPA level, should be identically equal to $\langle 2S^z\rangle_{\rm HF}$. This is becasue both the RPA and HF approximations are O(1) within the inverse-degeneracy expansion scheme [4] in powers of $1/\mathcal{N}$ ($\mathcal{N}$ is the number of orbitals per site), and therefore become exact in the limit $\mathcal{N}\to\infty$, when all corrections of order $1/\mathcal{N}$ or higher vanish. This is indeed confirmed as shown in Figs. 1 and 2. The deviation at small U is because of the neglect in Eq. (2) of the contribution from the single particle excitations across the charge gap, arising from the imaginary part of $\chi^0(\omega)$ in Eq. (1).

The sum $\langle S^+S^- + S^-S^+\rangle_{\rm RPA}$ yields a measure of transverse spin fluctuations about the HF state, and in the strong coupling for spin S, one obtains $\langle S^+S^- + S^-S^+\rangle_{\rm RPA} = (2S)\sum_q 1/\sqrt{1-\gamma_q^2}$. [4,16] Using the identity, $\langle S^zS^z\rangle = S(S+1) - \langle S^+S^- + S^-S^+\rangle/2$ in this limit, the sublattice magnetization $m=\langle 2S^z\rangle$ is then obtained from,

$$\langle S^z\rangle = S\left[1-\frac{1}{S}\left(\frac{\langle S^+S^-+S^-S^+\rangle}{2S}-1\right)\right]^{1/2} . \tag{4}$$

To order $1/2S$, this yields the correction to the sublattice magnetization of $(2S)^{-1}\sum_q[(1-\gamma_q^2)^{-1/2}-1] = 0.156$ and 0.393 for $S=1/2$ in three and two dimensions, respectively. This same result at one loop level was also obtained from a different approach in terms of the electronic spectral weight transfer, [3,4] and is in exact agreement with the SWT result. [16,17]

As $\langle S^z\rangle_{\rm HF}$ is the maximum (classical) spin polarization in the z-direction, and therefore also the maximum eigenvalue of the local S_z operator, therefore for arbitrary U, the HF magnitude $\langle S^z\rangle_{\rm HF}$ plays the role of the effective spin quantum number, S. The sublattice magnetization m is therefore obtained from $m = m_{\rm HF} - \delta m_{\rm SF}$, where the first-order, quantum spin-fluctuation correction $\delta m_{\rm SF}$ is obtained from Eq. (4) with $S=\langle S^z\rangle_{\rm HF}$,

$$\delta m_{\rm SF} = \frac{\langle S^+S^-+S^-S^+\rangle_{\rm RPA}}{\langle S^+S^- - S^-S^+\rangle_{\rm RPA}} - 1. \tag{5}$$

In the strong coupling limit $U/t\to\infty$, $\langle S^+S^- - S^-S^+\rangle_{\rm RPA} = \langle 2S^z\rangle_{\rm HF} = 1$ for $S=1/2$, so that the spin-fluctuation correction simplifies to, $\delta m_{\rm SF} = 2\langle S^-S^+\rangle_{\rm RPA}$. For a site on the B sublattice, where $\langle S^+S^- - S^-S^+\rangle_{\rm RPA} = \langle 2S^z\rangle_{\rm HF} = -1$, we have $\delta m_{\rm SF} = 2\langle S^+S^-\rangle_{\rm RPA}$.

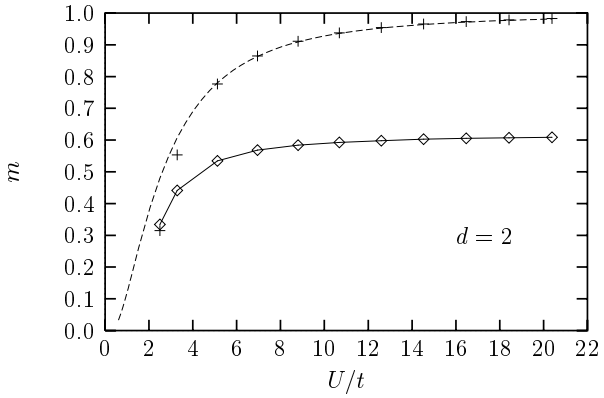

FIG. 1. The sublattice magnetization m vs. U in two dimensions (diamonds), along with the HF results from (i) the self-consistency condition (dashed), and (ii) $\langle 2S_z\rangle_{\rm HF} = \langle S^+S^- - S^-S^+\rangle_{\rm RPA}$ (plus).

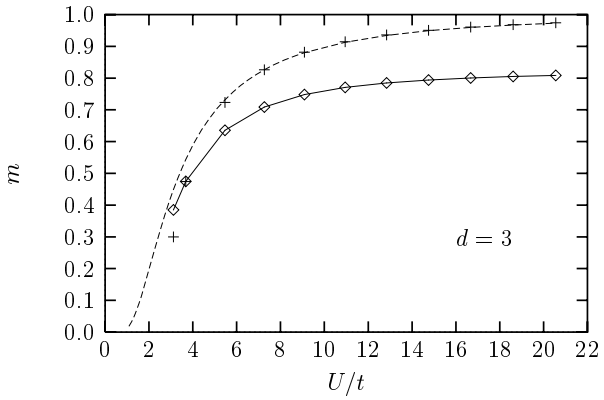

FIG. 2. The sublattice magnetization m vs. U in three dimensions (diamonds), along with the HF results from (i) the self-consistency condition (dashed), and (ii) $\langle 2S_z\rangle_{\rm HF} = \langle S^+S^- - S^-S^+\rangle_{\rm RPA}$ (plus).

The U-dependence of sublattice magnetization m is shown in Figs. 1, and 2 for $d = 2$ and $d = 3$, respectively. In both cases it interpolates properly between the weak and strong coupling limits, approaching the SWT results 0.607 and 0.844, respectively, as $U/t \to \infty$. A comparison of the m vs. U behaviour with earlier results is presented in Fig. 3 for the well studied $d = 2$ case. Earlier studies have employed a variety of methods including the variational Monte Carlo (VMC), [19] self-energy corrections (SE), [18] quantum Monte Carlo (QMC), [20] functional-integral schemes, [21] the generalized linear spin-wave approximation (GLSWA), [22] and mapping of low-energy excitations to those of a QHAF with U-dependent, extended-range spin couplings. [23]

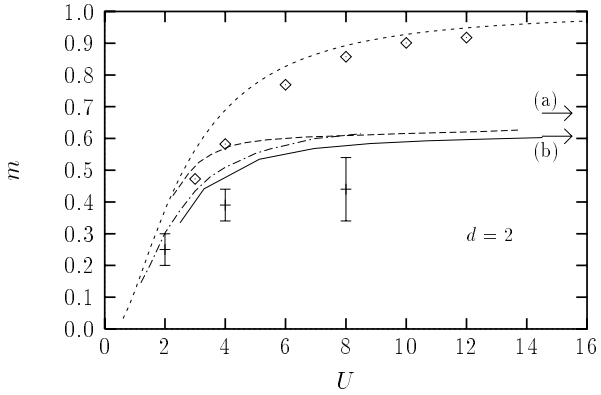

FIG. 3. The sublattice magnetization m vs. U from our RPA spin-fluctuation approach (solid line) compared with earlier results — VMC [19] (diamonds), SE [18] (dash-dot), QMC [20] (errorbars), and GLSWA [22] (dash). Also shown is the HF result (dotted). The arrows denote the asymptotic results of (a) [2] and (b) [1].

In addition to the two-sublattice basis, we have also used the full site representation in the strong coupling limit, in order to illustrate the scaling of the quantum correction with system size. Here the χ^0 matrix is evaluated and diagonalized in the site basis for finite lattices. Results for lattice sizes with $8 \le L \le 16$ are shown in Fig. 4. A quadratic least-square fit is used to extrapolate to infinite system size, which yields $\delta m_{\rm SF}(1/L \to 0) = 0.39$, in agreement with the result from Eq. (4).

IV. SPIN VACANCIES

The site representation has also been used to obtain transverse spin fluctuations for the problem of spin vacancies in the AF in the limit $U/t \to \infty$. As mentioned already this method is applicable in the whole range of vacancy concentration, and allows determination of the critical vacancy concentration at which the AF order parameter vanishes. For the vacancy problem we consider the following Hamiltonian on a square lattice with nearest-neighbor (NN) hopping,

$$H = -\sum_{<ij>\sigma} t_{ij}(a^\dagger_{i\sigma}a_{j\sigma} + \text{h.c.}) + U\sum_i \hat{n}_{i\uparrow}\hat{n}_{i\downarrow}\ , \qquad (6)$$

where the hopping terms $t_{ij} = 0$ if sites i or j are vacancy sites, and $t_{ij} = t$ otherwise. Thus, for a vacancy on site i, all hopping terms t_{ij} connecting i to its NN sites j are set to zero. The vacancy site is thus completely decoupled from the system. Half-filling is retained by having one fermion per remaining site. We consider the $U/t \to \infty$ limit, where the local moments are fully saturated, and the vacancy problem becomes identical to the

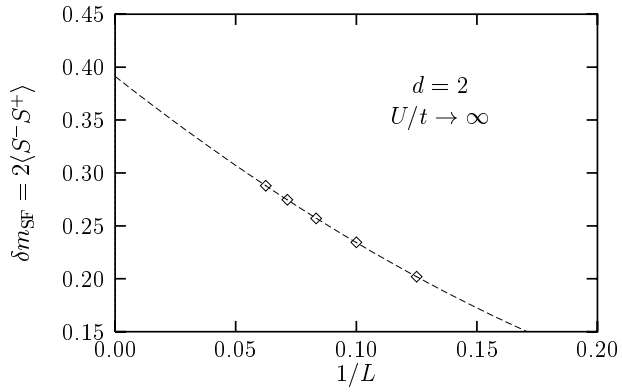

FIG. 4. The spin-fluctuation correction to sublattice magnetization $\delta m_{\rm SF}$ vs. $1/L$, for $L = 8$, 10, 12, 14, 16.

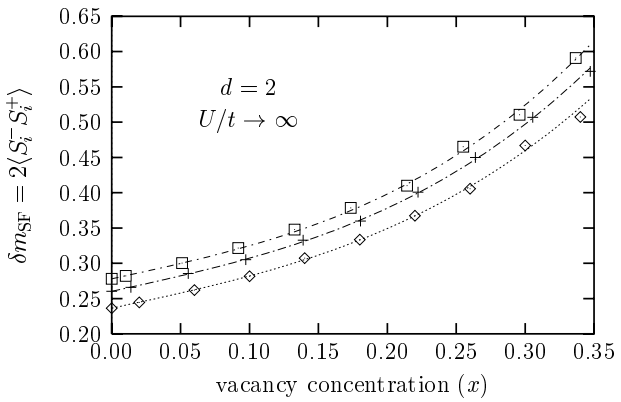

FIG. 5. The spin-fluctuation correction to sublattice magnetization $\delta m_{\rm SF}$ vs. x, for $L = 10$ (diamonds), 12 (plus), and 14 (squares).

spin-vacancy problem in the QHAF. This is also equivalent to the problem of non-magnetic impurities in the AF in the limit of the impurity potential $V \to \infty$. [14,15]

The structure of the $\chi^0(\omega)$ matrix in the host AF, and the modification introduced by spin vacancies has been considered earlier in the context of static impurities. [15] As the Goldstone mode is preserved, it is convenient to work with the matrix $K \equiv U[1 - U\chi^0]$, inverse of which yields the spin propagator in Eq. (1) near the mode energies. When expressed in units of $U^2t^2/\Delta^3 = 2J$, where $2\Delta = m_{\rm HF}U$ is the AF gap parameter, and $J = 4t^2/U$, it has the following simple structure for the host AF:

$$\begin{aligned} K^0_{ii} &= 1 + \omega \quad && i \text{ in A sublattice} \\ K^0_{ii} &= 1 - \omega \quad && i \text{ in B sublattice} \\ K^0_{ij} &= 1/4 \quad && j \text{ is NN of } i. \end{aligned} \tag{7}$$

Vacancies introduce a perturbation in K due to absence of hopping between the vacancy and NN sites, and we take $\delta K \equiv -U^2\delta\chi^0$ to refer to this vacancy-induced perturbation, so that $K = K^0 + \delta K$. If site i is a vacancy site and j the NN sites, then the matrix elements of δK are,

$$\delta K_{ij} = \delta K_{ji} = \delta K_{jj} = -1/4\,, \tag{8}$$

and the magnitude of K_{ii} is irrelevant since the vacancy site i is decoupled. Thus $K_{ij} = 0$, reflecting the decoupling of the vacancy, and the static part of the diagonal matrix elements K_{jj} on NN sites are reduced by $1/4$. For n vacancies on NN sites, the static part is $1 - n/4$. This ensures that the Goldstone mode is preserved. Thus if a spin on site j were surrounded by a maximum of four vacancies on NN sites, then the static part vanishes, and $K_{jj} = \pm\omega$, representing an isolated spin, which yields a $1/\omega$ pole in the transverse spin propagator. This is an isolated single-spin cluster, and with increasing vacancy concentration, larger isolated spin clusters are formed. As these are decoupled from the remaining system, their spin-fluctuation contributions are not included, as the OP vanishes for finite spin clusters. When x exceeds the percolation threshold ~ 0.4, the fraction of macroscopically large spin clusters in the system vanishes, and therefore no AFLRO is possible for $x > 0.4$.

For a given vacancy concentration and system size, the appropriate number of vacancies are placed randomly across the lattice, and the matrix K constructed accordingly. Exact diagonalization of K is carried out, and the eigensolutions are used to compute the transverse spin correlations from Eq. (2). The quantum, spin-fluctuation correction is then obtained from the strong-coupling limit of Eq. (5). The transverse spin correlation $\langle S^- S^+\rangle$ is averaged over all spins within the A sublattice. As mentioned already, only the spins in the macroscopic cluster spanning the whole lattice are considered, and contributions from spins in isolated spin clusters are excluded. Configuration averaging over several realizations of the vacancy distribution is also carried out.

The quantum spin-fluctuation correction vs. vacancy concentration is shown in Fig. 5 for three lattice sizes, $L = 10, 12, 14$. Best fits are obtained with an expression including a cubic term, $\delta m_{\rm SF} = \alpha + \beta x + \gamma x^3$. For the three lattice sizes α =0.236, 0.260 and 0.278, respectively, and as shown in Fig. 3, it extrapolates to 0.39 as $1/L \to 0$. The coefficient of the linear term is found to be nearly independent of system size, $\beta \approx 0.42$. And the cubic term γ takes values approximately 3.6, 4.0, and 4.4 for the three lattice sizes, and extrapolates to about 6.5 as $1/L \to 0$. With these coefficients, the spin-fluctuation correction $\delta m_{\rm SF}$ is nearly 1 for $x = 0.4$. Beyond $x = 0.4$, the percolation limit, there is no single, macroscopically large spin cluster left in the system. Therefore the point where the AF order parameter vanishes and AFLRO is destroyed due to spin fluctuations nearly coincides with the percolation threshold. This is in agreement with

results from series expansion [24] and quantum Monte Carlo simulations [25] of the QHAF with spin vacancies.

V. RANDOM-U MODEL

We now consider a quenched impurity model with a random distribution of impurity sites characterized by a local Coulomb interaction $U' \neq U$ for the host sites. With H and I referring to the sets of host and impurity sites respectively, we consider the following Hubbard model in the particle-hole symmetric form at half-filling and on a square lattice,

$$H = -t \sum_{<ij>\sigma} (a^\dagger_{i\sigma} a_{j\sigma} + \text{h.c.}) + U \sum_{\text{i}\in\text{H}} (n_{i\uparrow} - \frac{1}{2})(n_{i\downarrow} - \frac{1}{2}) + U' \sum_{\text{i}\in\text{I}} (n_{i\uparrow} - \frac{1}{2})(n_{i\downarrow} - \frac{1}{2}). \quad (9)$$

The motivations for studying this impurity model are threefold. In view of the observed *enhancement* of magnetic order at low concentration of impurities, [6] we shall analyze the suppression of quantum spin fluctuations to examine whether this is due to a local suppression at the low-U sites. The RPA evaluation of transverse spin correlations is also extended to the case of site-dependent interactions. Furthermore, at half-filling this model also provides a simplistic representation for magnetic impurity doping in an AF. This may appear contradictory in view of the apparently nonmagnetic ($U' \approx 0$) nature of the impurity sites. However, this feature is expressed only away from half-filling. [6]

The atomic limit $t = 0$ provides a convenient starting point for further discussions. In the particle-hole symmetric form of Eq. (9), since not only local interaction terms, but the on-site energy terms are also modified (from $-U/2$ to $-U'/2$) at the impurity sites, therefore the energy levels for added hole and particle are $(-U/2, U/2)$ and $(-U'/2, U'/2)$ for host and impurity sites respectively. To order t^2, this impurity model therefore canonically maps to the following $S = 1/2$ Heisenberg model

$$H_{\text{eff}} = J \sum_{<ij>\in H} (\vec{S}_i.\vec{S}_j - \frac{1}{4}) + J' \sum_{i\in I} \sum_{\delta} (\vec{S}_i.\vec{S}_{i+\delta} - \frac{1}{4}) \quad (10)$$

where in the first term $J = 4t^2/U$ is the conventional exchange coupling between neighboring host spins, and $J' = 8t^2/(U + U')$ is the exchange coupling between impurity spins and neighboring host spins. In writing Eq. (10) we have assumed the dilute impurity limit, and discounted the possibility of two impurity spins occupying NN positions, in which case the impurity-impurity exchange coupling will be $4t^2/U'$.

Therefore, in the strong correlation limit, this random-U model also describes magnetic impurities in the AF within an impurity-spin model. The magnetic-impurity doping is characterized by identical impurity and host spins ($S' = S$), but with different impurity-host exchange coupling ($J' \neq J$). Both cases $J' > J$ or $J' < J$ are possible, and in this paper we have considered the two cases: (i) $U' << U$ so that $J' \approx 2J$, and $U' = 3U$ so that $J' = J/2$. While this model is easily generalized to other magnetic-impurity models represented by locally modified impurity-host hopping terms $t' \neq t$, and/or different impurity energy levels, in fact, the essential features are already contained here as the impurity exchange coupling J' is the relevant quantity in determining the spin fluctuation behavior.

RPA with site-dependent interaction

We recast the RPA expression for the transverse spin propagator in a form suitable for site-dependent interactions. In terms of a diagonal interaction matrix $[U]$, with elements $[U]_{ii} = U_i$, the local Coulomb interaction at site i, the time-ordered transverse spin propagator at the RPA level can be rewritten, after simple matrix manipulations, as

$$[\chi^{-+}(\omega)] = \frac{[\chi^0(\omega)]}{1 - [U][\chi^0(\omega)]} = \frac{1}{[A(\omega)]} - \frac{1}{[U]} \quad (11)$$

where $[A(\omega)] = [U] - [U][\chi^0(\omega)][U]$ is a symmetric matrix. As $[U]$ is non-singular, the singularities in $[\chi^{-+}(\omega)]$, which yield the magnon modes, are then given completely by the vanishing of the eigenvalues of the matrix $[A]$. In terms of λ_n and $|\phi_n\rangle$, the eigenvalues and eigenvectors of the matrix $[A]$, we have $[A(\omega)]^{-1} = \sum_n \lambda_n(\omega)^{-1} |\phi_n(\omega)\rangle\langle|\phi_n(\omega)|$, so that the magnon-mode energies ω_n are then given by $\lambda_n(\omega_n) = 0$, and in analogy with Eq. (2) the transverse spin correlations are obtained from,

$$\langle S^-_i(t) S^+_j(t')\rangle_{\text{RPA}} = \pm \sum_n \frac{\phi^i_n(\omega_n)\phi^j_n(\omega_n)}{(d\lambda_n/d\omega)_{\omega_n}} \; e^{i\omega_n(t-t')}. \quad (12)$$

As we are interested in the dilute behaviour, we examine the correction to sublattice magnetization due to two impurities, one on each sublattice for symmetry. Since $m = m_{\text{HF}} - \delta m_{\text{SF}}$, corrections to both m_{HF} and δm_{SF} are expressed in the dilute limit (impurity concentration x) as $m_{\text{HF}} = m^0_{\text{HF}} - \alpha_{\text{HF}} x$, and $\delta m_{\text{SF}} = \delta m^0_{\text{SF}} - \alpha_{\text{SF}} x$. The overall $m(x)$ behavior therefore depends on the relative magnitude of the coefficients α_{HF} and α_{SF}. For $U = 10$ and $U' = 2$ we find, at the HF level, that $m^0_{\text{HF}} = 0.93$ and $\alpha_{\text{HF}} = 0.19$, both quite independent of system size.

The (site-averaged) spin fluctuation correction δm_{SF} is obtained from Eq. (5) with and without impurities, and the impurity contribution extracted. For $U' = 2$ we find a net *reduction* in δm_{SF}. Divided by $2/N$, the impurity concentration, this yields the coefficient α_{SF} defined

above, and also the per-impurity contribution to the total spin fluctuation correction over the whole lattice. The spin-fluctuation correction $\delta m_{\rm SF}$ for the pure case, and the per-impurity contribution ($\alpha_{\rm SF}$) are shown in Fig. 6 for different lattice sizes, along with least-square fits. It is seen that in the infinite size limit, the per-impurity reduction is nearly 0.2, which is more than half of the correction per site in the pure case (0.35). Thus, there is a substantial reduction in the averaged spin fluctuation correction due to the low$-U$ impurities.

As the two coefficients $\alpha_{\rm HF}$ and $\alpha_{\rm SF}$ are very nearly the same, the sublattice magnetization

$$m(x) = m(0) - (\alpha_{\rm HF} - \alpha_{\rm SF})x \tag{13}$$

shows negligible concentration dependence. Thus the (relatively small) reduction in the HF value due to the low-U impurities is almost fully compensated by the (relatively substantial) reduction in the spin fluctuation correction. To first order in x, we thus find that there is nearly no loss of AF order due to the low-U impurities. As mentioned earlier, even a slight enhancement in the AF order was recently seen for the case $U' = 0$. [6]

We next examine the site-dependence of the local spin fluctuation corrections $\delta m^i_{\rm SF}$ near the impurities. Table I shows that spin fluctuation is actually *enhanced* on the low-U impurity sites. The suppression of $\delta m^i_{\rm SF}$ in the vicinity more than compensates for this local enhancement, resulting in an overall reduction on the average. On the other hand, for $U' = 30$, we find that the correction is suppressed on the high-U impurity site, while it is enhanced on the average. Thus, to summarize, when the impurity spin is coupled more strongly (weakly), the spin-fluctuation correction is enhanced (suppressed) locally at the impurity site, but the average correction to sublattice magnetization is suppressed (enhanced).

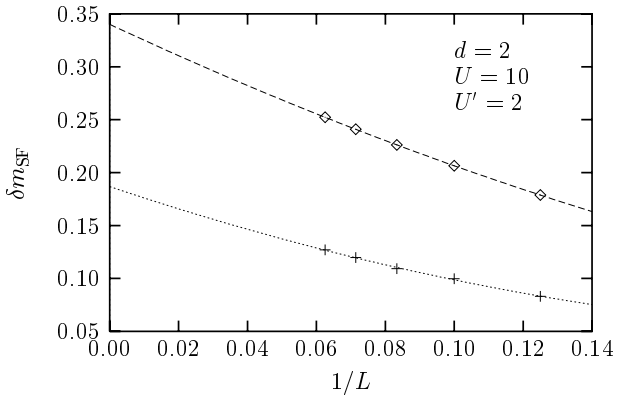

FIG. 6. The per-impurity reduction in the spin-fluctuation correction to sublattice magnetization $\delta m_{\rm SF}$ vs. $1/L$ (plus), for finite lattices with $L = 8, 10, 12, 14, 16$. Also shown is the correction per site for the pure system (diamonds), indicating significant relative impurity contribution.

This local enhancement can be understood in terms of the correlations $\langle S^-_i S^+_i \rangle$ as follows. Since the impurity spin is more strongly coupled to the neighboring spins, the NN matrix elements $A_{i\delta}$ are enhanced. This puts more magnon amplitude ϕ on the impurity site, so that from Eq. (2) the transverse spin correlations $\langle S^-_i S^+_i \rangle$, and therefore the spin-fluctuation correction, are enhanced for low-U impurities. The overall decrease in the averaged fluctuation correction, however, is due to the stiffening of the magnon spectrum in the important low-energy sector, following from the increased average spin coupling.

TABLE I. The local spin-fluctuation corrections $\delta m^i_{\rm sf}$ for a 16×16 system ($U = 10$), with two impurities at (11,4) and (4,14). For the two cases $U' = 2$ ($J' \approx 2J$) and $U' = 30$ ($J' = J/2$), quantum corrections are enhanced/suppressed locally at the impurity sites (indicated in boldfaces), but are suppressed/enhanced on the average.

site	1	2	3	4	5	6	7	8	9	10	11	12	13	14	15	16
1									.252	.251	.251	.251	.253	.252	.253	.251
2				$U' = 2$					.252	.252	.245	.253	.251	.253	.251	.253
3									.253	.241	.239	.240	.253	.251	.252	.252
4									.246	.239	**.295**	.239	.245	.251	.252	.251
5									.253	.241	.239	.241	.252	.251	.251	.252
6									.252	.253	.245	.252	.251	.251	.252	.250
7									.253	.252	.252	.252	.251	.252	.251	.252
8																
9																
10	.253	.253	.253	.253	.253	.253	.253	.253								
11	.253	.253	.253	.253	.254	.253	.253	.252								
12	.253	.254	.253	.261	.253	.254	.252	.253								
13	.253	.253	.265	.248	.265	.253	.254	.253								
14	.253	.261	.248	**.158**	.248	.261	.253	.253								
15	.254	.253	.264	.248	.265	.253	.253	.253			$U' = 30$					
16	.253	.253	.253	.260	.253	.253	.253	.253								

While these results also follow from the impurity-spin picture, the small charge gap at the impurity site does have an impact on the magnon spectrum. Within the localized spin picture, the highest-energy magnon mode corresponding to a local spin deviation at the impurity site would cost energy $4 \times J'/2 = 16t^2/(U + U')$. However, the highest energy in the magnon spectrum is actually seen to be $1.05t$, which is substantially smaller than $2J' = 1.33t$. This shows the compression effect of the low charge gap ($2.75t$) on the magnon spectrum. [26]

In conclusion, using a convenient numerical method for evaluating transverse spin correlations at the RPA level, quantum spin-fluctuation corrections to sublattice magnetization are obtained for the half-filled Hubbard model in the whole U/t range. Results in two and three dimensions are shown to interpolate properly between both the weak and strong correlation limits, and approach the SWT results as $U/t \to \infty$. The method is readily extended to other situations of interest involving defects in the AF, such as vacancies/impurities/disorder. Numerical diagonalization for finite lattices, along with finite-size scaling tested with the pure Hubbard model, allows for exact treatment of defects at the RPA level. This is illustrated with a study of the defect-induced enhancement/suppression in transverse spin fluctuations for spin vacancies and low-U impurities in two dimensions. While the quantum spin fluctuation correction to sublattice magnetization is sharply enhanced by spin vacancies, it is strongly suppressed by the low-U impurities, although the fluctuation correction is enhanced at the low$-U$ sites.

ACKNOWLEDGMENTS

Helpful conversations with D. Vollhardt and M. Ulmke, and support from the Alexander von Humboldt Foundation through a Research Fellowship at the Universität Augsburg are gratefully acknowledged.

[1] J. D. Reger and A. P. Young, Phys. Rev. B **37**, 5978 (1988).
[2] J. Carlson, Phys. Rev. B **40**, 846 (1989).
[3] A. Singh and Z. Teśanovič, Phys. Rev. B **41**, 614 (1990); Phys. Rev. B **41**, 11 457 (1990).
[4] A. Singh, Phys. Rev. B **43**, 3617 (1991).
[5] A. Singh, Report No. cond-mat/9802047, and references therein.
[6] P. J. H. Denteneer, M. Ulmke, R. T. Scalettar, and G. T. Zimanyi, Physica A **251**, 162 (1998); M. Ulmke, P. J. H. Denteneer, R. T. Scalettar, and G. T. Zimanyi, Report No. cond-mat/9707068.
[7] A. Singh, M. Ulmke, and D. Vollhardt, Phys. Rev. B **58**, 8683 (1998).
[8] B. Keimer, A. Aharony, A. Auerbach, R. J. Birgeneau, A. Cassanho, Y. Endoh, R. W. Erwin, M. A. Kastner, and G. Shirane, Phys. Rev. B **45**, 7430 (1992).
[9] E. Manousakis, Phys. Rev. B **45**, 7570 (1992).
[10] N. Bulut. D. Hone, D. J. Scalapino, and E. Y. Loh, Phys. Rev. Lett. **62**, 2192 (1989).
[11] W. Brenig and A. Kampf, Phys. Rev. B **43**, 12 914 (1991).
[12] C. C. Wan, A. B. Harris and D. Kumar, Phys. Rev. B **48**, 1036 (1993).
[13] D. Poilblanc, D. J. Scalapino, and W. Hanke, Phys. Rev. Lett. **72**, 884 (1994).
[14] P. Sen, S. Basu and A. Singh, Phys. Rev. B **50**, (RC) 10381 (1994).
[15] P. Sen and A. Singh, Phys. Rev. B **53**, 328 (1996).
[16] P. W. Anderson, Phys. Rev. **86**, 694 (1952).
[17] T. Oguchi, Phys. Rev. **117**, 117 (1960).
[18] J. R. Schrieffer, X.-G. Wen, and S.-C. Zhang, Phys. Rev. B **39**, 11663 (1989); **41**, 4784(E) (1990).
[19] H. Yokoyama and H. Shiba, J. Phys. Soc. Jpn. **56**, 3582 (1987).
[20] J. E. Hirsch and S. Tang, Phys. Rev. Lett. **62**, 591 (1989).
[21] H. Hasegawa, J. Phys. Cond. Matter **1**, 9325 (1989), and references therein.
[22] B. Mehlig and P. Fulde, Z. Phys. **94** 335, (1994).
[23] M. A. Tusch, Y. H. Szczech, and D. E. Logan, Phys. Rev. B **53**, 5505 (1996).
[24] C. C. Wan and A. B. Harris, J. Appl. Phys. **69**, 5191 (1991).
[25] J. Behre and S. Miyashita, Report No. cond-mat/9305004.
[26] P. Sen and A. Singh, Phys. Rev. B **48**, 15 792 (1993).